Report Title:

COAL AND CHAR STUDIES BY ADVANCED EMR TECHNIQUES

Report Type:	FINAL	Reporting Period Start Date: 09/01/1996	End Date: 02/29/2000

Principal Author(s): R. Linn Belford
Robert B. Clarkson
Mark J. Nilges
Boris M. Odintsov
Alex I. Smirnov

Report Issue Date: 04/30/2001

DOE Award No.: DE- FG22 -96PC96205

Submitting Organization(s)

Name & Address

University of Illinois at Urbana-Champaign
Department of Chemistry - Box 18-6 CLSL - MC712
600 S. Mathews
Urbana, IL 61801

(1)

(2)

(3)

(4)

(5)

COAL AND COAL CONSTITUENTS STUDIES BY ADVANCED EMR TECHNIQUES

by R. Linn Belford, Robert B. Clarkson, Mark J. Nilges, Boris M. Odintsov, and Alex I. Smirnov
University of Illinois at Urbana-Champaign

DISCLAIMER

ABSTRACT

Advanced electronic magnetic resonance (EMR) as well as nuclear magnetic resonance (NMR) methods have been used to examine properties of coals, chars, and molecular species related to constituents of coal. During the span of this grant, progress was made on construction and applications to coals and chars of two high frequency EMR systems particularly appropriate for such studies - 48 GHz and 95 GHz electron magnetic resonance spectrometer, on new low-frequency dynamic nuclear polarization (DNP) experiments to examine the interaction between water and the surfaces of suspended char particulates in slurries, and on a variety of proton nuclear magnetic resonance (NMR) techniques to measure characteristics of the water directly in contact with the surfaces and pore spaces of carbonaceous particulates.

TABLE OF CONTENTS

EXECUTIVE SUMMARY

The main advanced magnetic resonance methods employed over the period of this project were (1) W-band (100 GHz) electronic magnetic resonance (EMR) spectroscopy to provide an analytical tool to discriminate among very similar chemical species that are constituents of coals and closely related materials such as chars, (2) construction of a U-band (50 GHz) EMR spectrometer to aid such analysis by filling the wide gap between W-band and the lower available frequencies, (3) very low frequency pulsed dynamic nuclear polarization (DNP) spectroscopy for study of the interfaces between coal-like particles and the water medium in which they are suspended, and (4) a variety of proton nuclear magnetic resonance (NMR) techniques to measure characteristics of the water in contact with particle surfaces and pore spaces.

This project was carried out over a forty-two month period. Six individual project reports to the DOE described the instrumentation, techniques, theory, and typical results.[1-6] Sixteen peer-reviewed articles[7-22] contain details and discussions of parts of this work.

These reports describe the first observations of solid-liquid electron spin density transfer,

showing a transient chemical interaction between water molecules and particulate surfaces in an aqueous slurry of carbonaceous char particles by a proton pulsed Dynamic Nuclear Polarization (DNP) technique at low magnetic field. In a second study, by use of Fourier Transform Pulsed-Field-Gradient spin-echo NMR spectroscopy several self-diffusion coefficients were obtained in aqueous char suspensions corresponding to different mobilities of water molecules in the porous structures. It was concluded that the short-range nuclear-electronic interactions in pore space have the dominant effect on DNP enhancement in char suspensions. In another study, a strong particle size influence on NMR transverse proton relaxation in aqueous suspensions of these newly synthesized chars was found.

Multifrequency EMR spectroscopy can be a powerful tool in understanding details of the chemical species present in native and processed coals, coal constituents, and synthetic carbonaceous materials like chars. High frequency EMR is especially informative because of its ability to resolve species not distinguishable by conventional EMR. As part of this DOE project, two high frequency EMR spectrometers - a 48 GHz (U-band) and an improved 95 GHz (W-band) became fully operational. Design, construction, and performance information are available in the semiannual technical reports from this project. A comparative multifrequency study on fusinite demonstrated the power of HF EMR method in studies of carbonaceous solids. In particular, we studied the effect of oxygen on the fusinite EPR spectrum. The conventional EMR X-band (low frequency) spectrum of fusinite is a single featureless line with a width responsive to oxygen concentration with a fast and slow rate components. The slow process, barely measurable from X-band, looks very different at W-band: in half an hour the line first becomes slightly distorted and then two components arise, change widths, and separate further. This behavior can be well modeled and separated under a dipolar fitting model. One could say that X- and W-band experiments contradict each other: while the X-band spectrum is narrowing in the course of a continuous deoxygenation, the W-band spectrum (overall peak-to-peak line width measured as distance between maximum and minimum) is actually broadening. We speculate that oxygen serves as a bridge for spin exchange in fusinite.

INTRODUCTION

The interactions of water with coal are important factors in all aspects of coal cleaning and utilization. It has long been suspected that water adsorbed in the pores of the coal matrix effects the EPR spectral line shapes seen by advanced Electron Magnetic Resonance (EMR) methods. Recently, we developed a very low-field pulsed dynamic nuclear polarization (DNP) spectrometer capable of observing the interactions of water with the surfaces of carbonaceous solids. Some of the accomplishments of this project include use of the DNP method to determine the nature of water -surface interactions in aqueous char slurries.

EMR spectroscopy on coals and chars usually utilizes the rich population of unpaired electrons (typically, about 10^{19} unpaired electrons per gram) in these materials as reporters on their chemistry and local structures. Unfortunately, these materials usually display rather broad featureless spectra in conventional 9 GHz EMR experiments. Multifrequency, multifield EMR can help a great deal. Therefore, two higher-field instruments, at 48 GHz and 95 GHz, were constructed and refined as part of the DOE project, and test examples of applications to coal components, chars, and metal ions (often found in coal structures) were carried out.

MEASUREMENTS AND FINDINGS

Organization: This section of the Final Report summarizes the measurements activities covered in the six semiannual Technical Reports of this DOE project. For more details, see the individual reports.[1-6]

Dynamic Nuclear Polarization and NMR Measurements: For the first year of this grant (9/1/96-8/31/97), this research group reported on a new and exciting (EMR) electron magnetic resonance measurement technique, namely, very low frequency, low magnetic field, proton pulsed DNP (dynamic nuclear polarization) spectroscopy, for study of the interfaces between carbonaceous particles and the liquid medium in a slurry.[1] In DNP, unpaired electrons are spin-polarized by EMR rf absorption, and some of that magnetization is transferred to a nuclear spin system. An NMR frequency sweep reveals a positively or negatively enhanced NMR signal. Specifically, the first and second Technical Reports described the first observations of solid-liquid electron spin density transfer in an aqueous system consisting of hardwood char particles suspended in water — by a proton pulsed DNP technique at low magnetic field, 117 G. Samples of chars were obtained from various kinds of woods (e.g. hardwoods, softwoods) and other organic materials by charring under H_2 and CH_4 flow. The samples were heated at the rate of 10^o C per hour according to a pre-selected heat treatment profile, with a maximum temperature ranging from 420-720^{o}C. Prior to measuring, chars were finely ground to a particle size of about 10 μm. The samples were suspended in water, and then bubbled with pure helium for 15 min. The EPR spectra of chars in water consisted of a single Lorentzian line with a peak-to-peak line width of about 0.5 G, and a typical free radical g-factor, close to the free electron value of 2.0023. Proton DNP enhancement was seen for aqueous suspensions of several newly synthesized types of chars, where both positive and negative Overhauser effects were detected in different samples. This was the first discovery of a transient chemical, as opposed to physical, interaction between surfaces of certain chars and the hydrogen atoms of water molecules in the bulk.

Subsequently,[2] temperature dependencies of the DNP parameters were also measured, and enthalpies of activation for chemical exchange, E_h, were obtained. By using Fourier Transform Pulsed-Field-Gradient spin-echo NMR spectroscopy, we obtained several self-diffusion coefficients in aqueous char suspensions. These coefficients correspond to different mobilities of water molecules in porous structures. Proton spin-lattice relaxation data generally confirm the results of molecular diffusion measurements. On the basis of the Torrey model, the influence of a "cage effect" on DNP enhancement in porous media was discussed. It was concluded that the short-range nuclear-electronic interactions in pore spaces exert the dominant effect on DNP enhancement in char suspensions.

NMR relaxation measurements in carbonaceous particle slurries reported and interpreted in the fourth and fifth semiannual Technical Reports[4,5] were performed at a Larmor ^{1}H frequency of 6 MHz at room temperature with a relaxometer NMR-07PC. The Carr-Purcell-Meiboom-Gill (CPMG) technique was employed to measure water proton transverse relaxation times with a 180^o pulse period, τ, from 10 ms down to 0.2 ms. Software was written to account for multi-exponential relaxation, in which the relaxation (echo-decay) curve was described as a sum of exponential components $A(t)/A(0)=\sum p_i F_i(t)$ with weighting coefficients p_i and $F_i(t) = \exp(-t/T_{2i})$. To avoid the possible influence of slightly non-exponential time dependencies of $F_i(t)$, only the

initial part of each component was used, with consecutive subtraction of the most slowly relaxing $F_i(t)$-components from the total curve. Relaxation times and relative intensities p_i of components were determined by linear least squares analysis. Data were averaged over 50 acquisitions with phase cycling with a 10 s recycle delay to avoid saturation. Experimental relaxation time measurement errors did not exceed 5%. High-resolution proton spectra were obtained with a pulsed FT NMR spectrometer model Tesla-BS-567A. In tests for effects by soluble paramagnetic species that might exist in the chars, char particle suspensions were leached in pure water for several hours, the water was extracted, and NMR proton relaxation times measured to compare with those of the original pure water and of the water in the char suspensions.

High Frequency EMR Instrumentation.[3,6] High field (HF) EMR, which usually refers to EMR at >90 GHz, among other specific advantages, provides an analytical tool to discriminate among very similar paramagnetic species that are constituents of coals and closely related materials such as chars. These species are difficult to identify from conventional EMR (X-band, 9.5 GHz) because of insufficient spectral resolution for radicals with similar g-factors. In addition, conditions for fast Heisenberg exchange are often fulfilled at this frequency, resulting in a featureless single-line EMR spectrum at 9.5 GHz. In contrast, at 95 GHz (W-band), the g-factor resolution is tenfold that at X-band and the experimental frequency usually exceeds the exchange frequency. This yields an information-rich spectrum.

The first Illinois 95 GHz (W-band) EMR spectrometer (Mark I) was designed and built as a technological research and development project under the NIH Research Resources program and became operational in 1988-9. At that time, it was one of only two 95 GHz spectrometers in the world. Briefly, Mark I has a heterodyne bridge design with reference arm and is equipped with a narrow bore Varian XL-200 superconducting magnet operating in persistent mode at 3.3608 T and an air-cooled scanning coil of 300 G range. Using this spectrometer, we observed a variety of EMR line shapes for different coal samples and different macerals separated from the same coal, thus indicating different chemical environment for the free radical species and, possibly, presence of different radicals in some samples. The Mark I spectrometer had somewhat limited capabilities; in particular a relatively narrow magnetic field scan range and variable temperature only down to 150 K. Furthermore, the probehead did not have a remote tuning arrangement, complicating operation and increasing the time needed for certain of the experiments.

At the same time, emerging interest in the use of EMR in studies of a wider range of centers such as transition metal ions (which are also common impurities in carbonaceous materials) at high magnetic fields demanded a new spectrometer capable of:
- broad range of sample temperatures from 36.6 C. down to 4 K; - broad (several Tesla) but still accurate (milli- and sub-milliTesla) magnetic field scan; - quantitative rotation of small (submillimeter) crystals; - capability for samples exhibiting long relaxation times (typical for coal samples) that usually result in rapid-passage EMR spectra; - stability in magnetic field scans and resonance frequency to a ppm level or better.

To meet all these challenges, we built a new W-band instrument (Mark II) and during the period of this DOE project, we completed substantial improvements to this spectrometer.[3] The enhanced Mark II W-band and a Varian E-12 X-band EMR spectrometer were used to study oxygenation interaction with fusinite. Spectroscopy was carried out in the customary manner,

with careful measurements of instrument parameters such as field, frequency, power, modulation. Samples were carefully deoxygenated, exposed to controlled atmospheres with measured oxygen partial pressures, and deoxygenated again while monitoring the EMR spectra as functions of time and O_2 level.

The work that we reported for the sixth half-year of this project[6] is design and construction of a new high-magnetic-field electron magnetic resonance spectrometer operating at an unusual microwave frequency, 48 gigahertz, corresponding to 6 mm wavelength. The purpose of this system is to fill the large gap between the shortest spectrometer wavelength of conventional commercial instrumentation, 10 mm, and the longest available, 3 mm, in our custom-design high-field spectrometers. This new capability will enable one to step systematically through a series of well-spaced wavelengths in order to follow, and aid in following and interpreting the evolution of spectral resolution in coals and chars as well as in many other materials. During Project Period 6, the 6 mm spectrometer bridge was designed, constructed, and tested together with electronic gear borrowed from another spectrometer. The electronics components dedicated to this spectrometer were under construction as Project Period 6 ended on 8/31/99, and this remaining task was subsequently finished in 2000 under a no-cost extension of the contract period. Some time during the no-cost extension period was also devoted to the development of a LODEMR (longitudinally detected electron magnetic resonance) technique for measuring short electron spin-lattice relaxation times,

RESULTS, DISCUSSION, and CONCLUSIONS

DNP and associated NMR studies.

In general, the unpaired electron spins used to dynamically polarize nuclei are distributed uniformly throughout the bulk of the sample. In some cases, DNP can be produced in a liquid by pumping with microwave radiation in resonance with paramagnetic centers near a solid-liquid interface. There are only a few reported experimental studies of solid-liquid DNP transfer between sublevels in magnetic spin systems consisting of species with different gyromagnetic ratios. Most of these have described the dominant "solid-state" DNP effect due to pure dipole-dipole intermolecular interactions, such as those observed between free radical labels immobilized on a surface and solvent protons, in contrast to the current work. In this study, the proton DNP enhancement of water molecules was observed in aqueous suspensions of several newly synthesized types of chars, where both positive and negative Overhauser effects were detected in different samples. Table 1 shows DNP parameters and proton spin-lattice relaxation times T_1 for chars suspended in water with different nuclear-electron interactions. [1] Notice particularly that A, the proton polarization enhancement factor, is positive for two chars manufactured from hardwoods. This strongly suggests a transient chemisorption of water on the carbonaceous particle surfaces, since the dipole-dipole interaction between water and surface electrons during diffusion leads to a negative A, while direct overlap of the electronic wave function and a surface-resident water proton would produce positive enhancement. From the difference between the experimental proton T_{1n} and T_{2n} relaxation times and DNP results, it is possible to estimate the contact hyperfine coupling constant at the solid-liquid interface $a = 5.3\times10^{-3}$ MHz. The values of the enthalpy of activation of chemical exchange E_h, as well as the hyperfine scalar constant a again strongly suggest the presence of weak chemisorption bonds at

the solid/liquid interface that are capable of facilitating the electronic delocalization whose effect is observed in these DNP experiments.

The temperature-dependent DNP effect seen in aqueous char suspensions is the result of a delicate balance between dipole-dipole and scalar interactions as well as the competition between corresponding correlation times at the solid/liquid interface. The translational diffusion of water molecules is responsible for d-d relaxation, which dominates at low temperatures. The scalar interaction is modulated mainly by electron spin relaxation and an isotropic proton-electron spin chemical exchange process on the surface.

A strong temperature dependence of the DNP enhancement was observed in aqueous suspensions of the hardwood chars (Fig.1-a). The increase in scalar polarization with temperature suggests the possibility of exchange processes at the solid-liquid interface. We constructed a model of molecular migration at the solid-liquid interface to account for these observations. In contrast to hardwood chars, the negative DNP enhancement in fructose-precursor char suspensions was practically temperature independent (Fig.1-b). suggesting that the frequency dispersion is negligible in these systems and that the "white spectrum" condition was realized in the frequency region investigated. Temperature independence of DNP enhancement in fructose char suspensions indicates also dominance of the dipole-dipole type of hyperfine interaction at solid-liquid interface, because the change in temperature must lead to a change in the balance between dipole-dipole and scalar solid-liquid interactions, as in the case of hardwood char suspensions (Figs. 1-4).

The sizes of the observed positive as well as negative DNP enhancements in char suspensions are more than an order of magnitude less than the theoretical maximum of pure scalar (+330; scalar relaxation of Abragam's Type II) and pure dipolar (-330) coupling, respectively. One possible mechanism responsible for the lower DNP enhancement in char suspensions is the inhomogeneous molecular diffusion and magnetic relaxation processes in porous media.

Self-diffusion coefficients, D, for aqueous char suspensions were measured by PFG spin-echo NMR spectroscopy. The near-linear dependence of $\ln(A_g/A_o)$ on the gradient strength was observed in fructose char suspensions (Fig. 2). It is an important feature of the data, as it indicates that the water molecules are dominantly undergoing unrestricted diffusion in this kind of chars. This observation may be caused by a *hydrophobic* surface character of the fructose chars. This is in good agreement with the dominant dipole-dipole (through space) type of solid-liquid hyperfine interactions, which leads to negative DNP enhancement in these char suspensions. In contrast to fructose char suspensions, the effect of restriction on the PFG-NMR diffusion measurement is clearly demonstrated by the data obtained for hardwood char suspensions (Fig. 2). The observation suggests the hydrophilic character of the surfaces of these chars with developed porous structures (Fig. 3). The hydrophilic character of chars is favorable to short-distance contact hyperfine coupling at solid-liquid interface, which leads to electron delocalization from paramagnetic centers on the char surface to water protons and to positive DNP enhancement in hardwood char suspensions (Table 1). Proton spin-lattice relaxation data generally confirm the results of molecular diffusion measurements. Our analysis of the data indicate that in hardwood char suspensions the fraction of the water molecules in pore spaces is equal to 12.2% in contrast to only 2% in fructose chars, suggesting an essential difference in the porous structure of these chars.

NMR relaxation studies. The additional NMR relaxation work to help furnish an understanding of molecular diffusion and spin dynamics at the solid-liquid interface in newly synthesized carbonaceous particulate materials (chars) suspended in water slurries involved both experiments (see "Measurements" section above) and theoretical modeling, as reported in the fourth and fifth semiannual Technical Reports.[4,5] Table 2 shows experimental proton transverse relaxation times $(T_2)_{obsd,\,i}$ for a range of particle sizes and several 180° pulse intervals, τ, in the CPMG NMR pulse sequence for aqueous char slurries.

The main conclusions of these DNP and related NMR studies of aqueous carbonaceous particle slurries are as follows:[1,2,4,5]

(1) Surfaces of certain types of char particles are sufficiently hydrophilic that a transient chemisorption of water creates an electron-proton contact interaction that dominates the through-space dipole-dipole interaction.

(2) The main DNP processes in char suspensions occur in pore spaces of chars, and the short-range nuclear-electronic interactions in porous structures dominate the DNP enhancement. Long-range interactions associated with the different kinds (nuclear and electron-nuclear) of relaxation processes in the reminder of the surface layer have small or even negligible effect.

(3) Synthesizing chars with substantially developed porous structures and small pore sizes, small tortuosity, and fast spin-lattice relaxation in the pore spaces leads to increased DNP effects in the char suspensions.

(4) A strong particle size influence on NMR transverse proton relaxation in aqueous suspensions of several newly synthesized carbon based chars was found.

(5) The dependence of the transverse relaxation of water protons on particle size in these suspensions of several newly synthesized carbon based chars can be interpreted quantitatively in terms of a two-stage molecular exchange model. A porous cage effect leads to slow exchange between molecules inside and outside pores in contrast to fast molecular exchange processes at the solid-liquid interface, where the usual two-site formalism can be applied. Owing to increasing surface-to-volume ratio, the corresponding transverse relaxation times of water protons in aqueous char suspensions are shortened as the size decreases.

(6) Surface properties strongly affect the relaxation times. The more the hydrophilic character of the surface, the shorter the relaxation times at the solid-liquid interface.

(7) The strong particle size effect on the transverse relaxation time of solvent protons seen in char suspensions makes possible the rapid and easy measurement of relative particle sizes in different kinds of suspensions by an NMR pulsed technique.

W-Band (95 GHz) and U-Band (48 GHz) EMR spectrometers and applications to coal science.

1. The Mark II W-band (95 GHz) EMR spectrometer.

The new Mark II W-band EMR spectrometer built at the University of Illinois outperforms its prototype in many respects. Briefly, Mark II features: ! an Oxford custom-built 7 T superconducting magnet which is scannable from 0 to 7 T at up to 0.5 T/min; ! water-cooled coaxial solenoid designed and built at the University of Illinois with up to ±550 G scan under digital (15 bits resolution) computer control; custom-engineered precision feed-back circuit based on an Ultrastab 860R sensor that has linearity better than 5 ppm and resolution of 0.05

ppm; ! an Oxford CF 1200 cryostat modified at the University of Illinois to accommodate a new W-band probehead with remote tuning and one-axis goniometer for vertical bore solenoid. Technical details and applications beyond the scope of this report are provided in our recent publications.

2. Recent upgrades of the Mark II W-band (95 GHz) EMR spectrometer.[3]

During the last year we have carried out several important upgrades to keep up with the challenges set up by the applications. Particularly we have: ! replaced the entire waveguide of the low temperature probehead with a flexible dielectric Goretex waveguide section; this upgrade provides superb cavity temperature insulation (important for cryogenic experiments with carbonaceous materials and polymers with metal ions), low microwave loss, and vacuum-tightness; thus, we no longer need a vacuum window on the top of the cryostat. The window caused microwave losses, reflections, and signal phase shift. This waveguide also is an attractive solution for λ-point EPR experiments; ! incorporated a low-noise 95 GHz amplifier (Millitech) which has 21.8 dB gain and 4.8 dB noise figure at 94.3 GHz; use of this amplifier in many cases eliminates rapid-passage conditions in cryogenic EPR experiments thus improving spectral resolution. (Long relaxation times and rapid passage conditions are typical for many organic free radicals and particularly coals at cryogenic temperatures.); ! developed a high Q ($\approx$4000) cylindrical resonator which provides high concentrational sensitivity for aqueous samples and slurries of carbonaceous materials comparable to that of traditional X-band EMR. In addition, we have carried out extensive tests of the Oxford magnet in order to characterize the hysteresis-like behavior during wide (several Teslas) scans. NMR and Hall-effect Gaussmeters as well as a high-speed current transducer have been used for tracking the magnetic field and current through the solenoid and their accuracy have been compared, in order to measure the field as accurately as possible. The non-linear hysteresis-like behavior was found to be repeatable, thus allowing the use of the current-feedback as one of the mechanisms in controlling magnetic field in experiments requiring several Tesla scans such as metal ion problems often require.

3. U-band (48 GHz) EMR spectrometer.[6]

Because of the large gap in wavelength between the 3-mm system summarized above and the conventional 10-mm and lower frequencies available commercially, it has often been difficult to track the origins of spectral features from the high to the low wavelength regions. Therefore, it was decided to design and construct an additional system operating at around 6 mm wavelength, in the microwave range designated "U band". The DOE funding was supplemented by an internal grant from the University of Illinois Research Board in order to allow this development to proceed. The new U-band (48 GHz) bridge has been constructed and is shown schematically in Figure 5. A specially designed low -noise Gunn oscillator source allows both mechanical and electrical tuning so as to provide for automatic frequency control (AFC). The bridge is designed to be mounted on a Varian E-line 15-inch magnet and to be used with a Varian E-15 EPR console. With the system just completed at the end of the no-cost extension period of this grant, it has not yet been put into standard service for examination of coals and chars. But excellent practical performance test examples are provided by complexed transition metal and rare earth S-state ions, S-state d^5 - Mn(II) - and f^7 - Gd(III) - systems. Figure 6 illustrates the variation of g_{eff} with inverse experimental frequency squared for Q-, U-, and W-band for some gadolinium (III) ions complexed to organic moieties. Theory predicts that the spectral center-of-gravity for S-state high-spin ions (from which a "g shift" is calculated) will vary with the zero-

field splitting (determined by the ions' surroundings) and with wavelength of the spectrometer. Moreover, over some range, the g-shift should be described adequately by second-order perturbation theory and should vary as the square of the wavelength (or square of the inverse frequency).

3. An Application of HF EMR to Coal Constituents.[6]

The third semiannual report[3] focused on fusinite to demonstrate the power of HF EMR methods in studies of carbonaceous solids. Fusinite, one of the most homogeneous of natural coal fractions, has a low level of inorganic impurities. We studied the effect of oxygen on the fusinite EMR spectrum, partly because, based on our recent magnetic susceptibility measurements, we had already speculated that O_2 might play a substantial role in spin-spin interactions in fusinite and other carbonaceous solids. Also, fusinite is now used as a probe to measure oxygen and nitric oxide concentrations *in vivo* and *in vitro*, and detailed understanding of oxygen effects on EMR spectrum are important for synthesizing new carbonaceous EMR probes for such purposes.

The conventional EMR X-band spectrum of fusinite is a single featureless line of width responsive to oxygen level. An example of such a spectrum for a carefully deoxygenated sample is shown in Fig.7 (A). The spectrum has broad wings which cannot be modeled by a Lorentzian function or inhomogeneous line shape model. These wings could be due to presence of several components with different T_2 but near-identical g-factor or to peculiarities of spin- spin interactions. For example, incompletely averaged dipole-dipole interaction is known to cause some extra broadening. A model of magnetically diluted solids in which dipolar broadening is much less than inhomogeneous line width, thus allowing an adiabatic approximation for the dipole-dipole interaction, was considered. It has been shown that in the high temperature limit, when dipole-dipole interaction is modulated by random spin flip-flops, the spin polarization effects are negligible, and the FID, $\upsilon_{FID}(t)$, is no longer a simple exponential but takes the form:

$$\upsilon_{FID}(t) \approx \exp(-a(t)^{1/2}), \qquad [1] \quad \text{where}$$

$$a = \frac{8\pi^{5/2}}{3^{5/2}}\langle g^2\rangle \beta^2 \hbar^{-1} C (T_1)^{1/2}, \qquad [2]$$

$\langle g^2 \rangle$ is a weighted g-factor for the two interacting species [13], C is spin concentration, and T_1 is the spin-lattice relaxation time. The corresponding CW spectrum $V(\omega)$ is given by a Fourier transform and is not Lorentzian; while the central part is slightly sharper than the Lorentzian for the same peak-to-peak line width $\Delta B_{p\text{-}p}$, the wings vanish less rapidly. As a result, dipolar broadening as given by eq. [1] decreases the peak-to-peak intensity of the CW spin-label spectrum by adding very broad wings with only a little broadening of the central part.

We used this model to fit the experimental spectrum using a fast convolution algorithm. In Fig.7, the fusinite X-band EMR spectrum is compared to least-squares simulations. They match closely. This exceptional fit demonstrates that the fusinite spectrum could be well described by a model of a single paramagnetic species with EMR line shape determined by spin exchange and dipole-dipole interaction. Under deoxygenation, the peak-to-peak fusinite line width initially decreases very rapidly with some further small changes observed over a period of a few hours (Fig. 8). The fast phase of deoxygenation is likely related to molecular oxygen removal from the fusinite porous structure; the slow phase could be related to a slower process

determined by oxygen diffusion in the carbonaceous particle matrix.

This slow process is barely discernible from X-band spectra but looks dramatically different at W-band (Fig. 9): in half an hour the line first becomes slightly distorted and then two components arise, change widths, and separate further. These two components can be well modeled and separated using the same dipolar fitting model we developed for the X-band fusinite spectrum (Fig. 10). One could say that X- and W-band experiments contradict each other: while the X-band spectrum is narrowing in the course of a continuous deoxygenation, the W-band spectrum (overall peak-to-peak line width measured as distance between maximum and minimum) is actually broadening. However, this puzzling behavior can be explained in terms of exchange theory and our hypothesis that molecular oxygen could serve as a bridge for those interactions. The line width of fusinite at X-band is primarily determined by both spin exchange and dipole-dipole interactions between the paramagnetic species in solid; the oxygen serves as an additional relaxer for these species and it causes some extra broadening also by the exchange mechanism. Complete deoxygenation does not break the existing exchange conditions (exchange frequency is higher than 9.5 GHz), so the spectrum remains unresolved while the width gradually decreases while oxygen is removed from the solid matrix and absorption sites. At W-band, the exchange frequency becomes lower than the frequency of the experiment as oxygen is removed from the system. We speculate that oxygen serves as a "bridge" for spin exchange; removing the oxygen thus decreases the effective exchange frequency. This causes the signals to split and to separate further in course of the experiment.

Additional support of this exchange condition can be deduced from other multifrequency EPR data, taken at the very initial stage of deoxygenation, which show that the line width actually drops a little from 1 to 9.5 GHz and then increases as the EMR frequency increases. This decrease is in accord with Anderson-Weiss theory, which predicts a decrease in the peak-to-peak line width for exchange-narrowed lines. At higher frequencies, the differences in g-factors cause an initial broadening which is proportional to $(\Delta g \cdot B)^2$ before lines begin to split.

Main conclusions of the W-Band and U-Band HF EMR projects: (1) A unique 3-mm band EMR spectrometer has been built and enhanced[3,15]; the high sensitivity and especially high spectral and temporal resolution that it makes possible will be of direct assistance in distinguishing between chemical structures in coals and chars and will allow kinetics of processes involving coals and chars to be studied with better specificity. (2) A unique 6-mm band EMR spectrometer has been designed and successfully built to exacting performance standards in order to bridge the large gap between conventional spectrometer wavelengths (3-10 mm) and existing high-field systems (<3 mm).[6] (3)) Clearly, as the data of Figure 6 show, the predicted linear relationship between g-shift and inverse frequency squared can be realized and accurate zero-field splitting constants for high-spin radicals or ions in solution or powders can be determined. (4) A W-band/X-band study of oxygenation and deoxygenation of a coal maceral, fusinite, reveals more than one signal component with different time dependences and demonstrates the power of HF EMR spectroscopy to identify multiple sites and elucidate rates and mechanisms of interactions of coal particles with their environment.

REFERENCES

1. R.L. Belford and R.B. Clarkson, "Coal and Coal Constituents Studies by Advanced EMR Techniques," *First Semiannual Report on DE-FG22-96PC96205,* March 31, 1997.

2. R.L. Belford, R.B. Clarkson, B.M. Odintsov, and P.J. Ceroke, "Coal and Coal Constituents Studies by Advanced EMR Techniques," *Second Semiannual Report on DE-FG22-96PC96205,* September 30, 1997.

3. R.L. Belford, R.B. Clarkson, Smirnov, A.I., and M.J. Nilges, "Coal and Coal Constituents Studies by Advanced EMR Techniques," *Third Semiannual Report on DE-FG22-96PC96205,* March 31, 1998.

4. R.L. Belford, R.B. Clarkson, and Odintsov, B.M., "Coal and Coal Constituents Studies by Advanced EMR Techniques," *Fourth Semiannual Report on DE-FG22-96PC96205,* September 30, 1998.

5. R.L. Belford, R.B. Clarkson, and B.M. Odintsov, "Coal and Coal Constituents Studies by Advanced EMR Techniques," *Fifth Semiannual Report on DE-FG22-96PC96205,* March 31, 1999.

6. R.L. Belford, R.B. Clarkson, and M.J. Nilges, "Coal and Coal Constituents Studies by Advanced EMR Techniques," *Sixth Semiannual Report on DE-FG22-96PC96205,* September 30, 1999.

7. Atsarkin, V. A., Demidov, V. V., Vasneva, G. A., Odintsov, B. M., Belford, R. L., Radüchel, B., Clarkson, R. B., "Direct Measurement of Fast Electron Spin-Lattice Relaxation: Method and Application to Nitroxide Radical Solutions and Gd^{3+} Contrast Agents," *J. Phys. Chem. A. 105*:9323-9327, 2001.

8. Odintsov, B.M., Temnikov, A.N., Belford, R.L., Ceroke, P.J., Clarkson, R.B. "Peculiarities in the Water Adsorption and Morphology of Carbon Chars Assessed by NMR", *J. Colloid & Interface Sci., 234:*137-141, 2001.

9. Clarkson, R.B., Ceroke, P.J., Norby, S.-W., Odintsov, B.M.,"Stable Particulate Paramagnetic Materials as Oxygen Sensors in EPR Oximetry," Chapter 7 in *Biological Magnetic Resonance, Vol. 20: In Vivo EPR, Theory and Applications,* L.J. Berliner & C. Bender, eds., Kluwer/Plenum Publishing, 2000.

10. Atsarkin, V.A., Vasneva, G.A., Demidov, V.V., Dzheparov, F.S., Odintsov, B.M., Clarkson., R.B. "Dipolar Broadening and Exchange Narrowing of EPR Lines from Paramagnetic Centers Distributed on a Solid Surface", JETP Letters. *72*:369-372, 2000.

11. Odintsov, B.M., Belford, R.L., Clarkson, R.B., "Hyperfine Interactions and Molecular

Dynamics in Carbon-Based Suspensions," *Recent Research Developments in Physical Chemistry*, *3*:459-474, 1999.

12. Odintsov, B.M., Belford, R.L., Ceroke, P.J., Temnikov, A.I., Kashaev, R.S., Clarkson, R.B., "Spin-Lattice Relaxation and NMR Spectroscopy in Aqueous Char Suspensions," *Colloid J.*, *62*:688-692, 2000.

13. Vartapet'yan, R.Sh., Clarkson R.B, Odintsov B.M., Filippov A.V., Skirda V.D. "Porous Structure of Active Carbons Determined from the Adsorption of Water Vapors and Melting of Water and Cyclohexane in Pores", *Colloid J.*,*62*:526-541, 2000.

14. Temnikov, A.N., Odintsov, B.M., Idiyatullin, Z.Sh., Clarkson, R.B., "Carbon Based Oxygen Biosensors," in *New Medical Techniques*, *6*:37-38, 1999.

15. Nilges, M.J., Smirnov, A.I., Clarkson, R.B., Belford, R.L., "Electron Paramagnetic Resonance W-Band Spectrometer with a Low Noise Amplifier," *Appl. Magn. Reson.*, 1999, *16*:167-184.

16. Odintsov, B.M., Temnikov, A.N., Idiyatullin, Z.Sh., Kashaev, R.S., Belford, R.L., Ceroke, P.J., Kuriashkin, I.V., Clarkson, R.B., "Particle Size Effect on Transverse NMR Relaxation in Aqueous Char Suspensions," *Colloids & Surfaces*, *157*:177-183, 1999.

17. Odintsov, B. M., Belford, R. L., Ceroke P.J., Idiyatullin, Z. S., Kashaev, R. S., Kuriashkin, I. V., Rukhlov, V.S., Temnikov, A. N., and Clarkson, R. B., "Molecular Diffusion and DNP Enhancement in Aqueous Char Suspensions", *J. Magn. Reson.*, *135*:435 - 443 ,1998.

18. Clarkson, R.B., Odintsov, B.M., Ceroke, P.J., Ardenkjaer-Larsen, J.H., Fruianu, M., Belford, R.L., "Electron Paramagnetic Resonance and Dynamic Nuclear Polarization of Char Suspensions: Surface Science and Oximetry," *Phys. Med. Biol.*, *43*:1907-1920, 1998.

19. Norby, S.W., Swartz, H.M., Clarkson, R.B., "Electron and Light Microscopy Studies on Particulate EPR Spin Probes Lithium Phthalocyanine, Fusinite, and Synthetic Chars," *J. Microscopy*, *192*:172-185, 1998.

20. Odintsov, B., Belford, R.L., Ceroke, P., Clarkson, R.B., "Solid-Liquid Electron Density Transfer in Aqueous Char Suspensions by ^{1}H Pulsed Dynamic Nuclear Polarization at Low Magnetic Field," J. Am. Chem. Soc., *120*:1076-1077, 1998.

21. Odintsov, B.M., Belford, R.L., Ceroke, P.J., Odintsov, A.B., Clarkson, R.B., "Temperature Dependence of Solid-Liquid Scalar Interactions in Aqueous Char Suspensions by Nonstationary DNP at Low Magnetic Field," *Surf. Sci.*, *393*:162-170, 1997.

22. Odintsov, B.M., Belford, R.L., Clarkson, R.B., "Cross-Relaxation in Electron-Nuclear Coupled Systems by Pulsed Dynamic Nuclear Polarization at Low Magnetic Fields," *J. Phys. Chem.*, *101*:116-121, 1996 .

TABLES AND FIGURES

Table 1. DNP/NMR data at magnetic field 117.5 G and molecular-kinetic parameters in aqueous suspensions of chars.

No	Material (pyrolysis atmosphere)	T_{1n}, s (300° K)	T_{2n}, s (300° K)	ΔT_n^{-1}, s^{-1}	f	A_{max} (360° K)	M	E_h, kcal/mole
1	Hardwood (CH_4)	0.58 ±0.03	0.08 ±0.004	10.78 ±0.05	0.75 ±0.04	+44 ±2.0	14.69 ±0.02	13.44 ±0.02
2	Hardwood (H_2)	0.47 ±0.03	0.09 ±0.004	8.98 ±0.05	0.8 ±0.04	+20 ±1.0	11.99 ±0.02	13.48 ±0.03
3	Softwood (H_2)	0.43 ±0.02	0.11 ±0.005	6.77 ±0.03	0.81 ±0.04	-28 ±1.5	9.41 ±0.03	14.12 ±0.03
4	Starch (H_2)	0.14 ±0.006	0.095 ±0.005	3.38 ±0.02	0.94 ±0.05	-32 ±1.6	4.7 ±0.02	14.21 ±0.03
5	Fructose (H_2)	0.17 ±0.008	0.120 ±0.006	2.45 ±0.01	0.93 ±0.05	-46 ±2.3	3.5 ±0.01	14.28 ±0.03

Table 2. Observed Proton Transverse Relaxation Time ($T_{2\ obsd,i}$, in sec) as Function of Particle Size and 180° Pulse Interval τ in CPMG Pulse Sequence in Aqueous Char Suspensions.

No.	Char particle size (μm)	τ, ms				
		0.2	1.0	2.0	5.0	10.0
1	850 ± 170	0.743 ± 0.04	0.722 ± 0.04	0.754 ± 0.04	0.741 ± 0.04	0.720 ± 0.04
2	450 ± 90	0.632 ± 0.03	0.624 ± 0.03	0.636 ± 0.03	0.651 ± 0.03	0.648 ± 0.03
3	250 ± 50	0.470 ± 0.02	0.495 ± 0.03	0.467 ± 0.02	0.432 ± 0.02	0.461 ± 0.02
4	100 ± 20	0.208 ± 0.01	0.210 ± 0.01	0.202 ± 0.01	0.213 ± 0.01	0.196 ± 0.01
5	50 ± 10	0.100 ±0.005	0.087	0.079 ±0.004	0.086 ±0.004	0.086 ±0.005

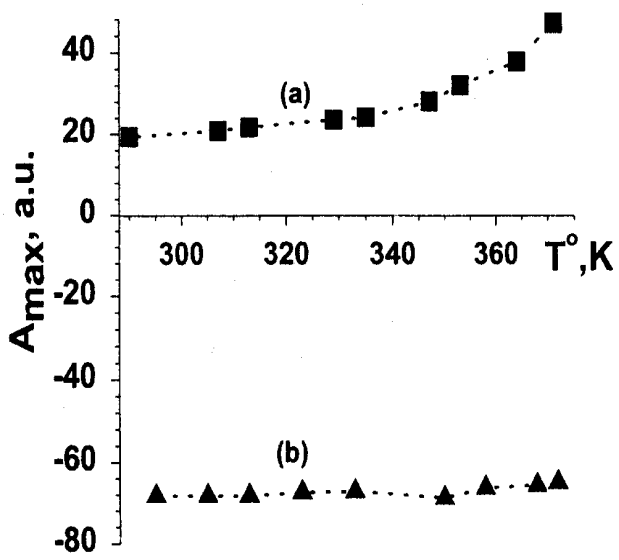

Fig. 1. Temperature dependence of DNP enhancements of water protons in aqueous suspensions of chars made from: a) hardwood and b) fructose. Instrument paramers: B_{1S}= 0.1G, τ_p= 0.5 s, τ_d = 4 ms.

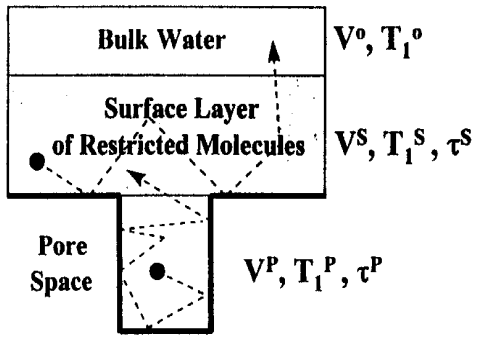

Fig. 3. Schematic illustrating the effect of restricting boundaries on water diffusion and relaxation measurements in char suspensions.

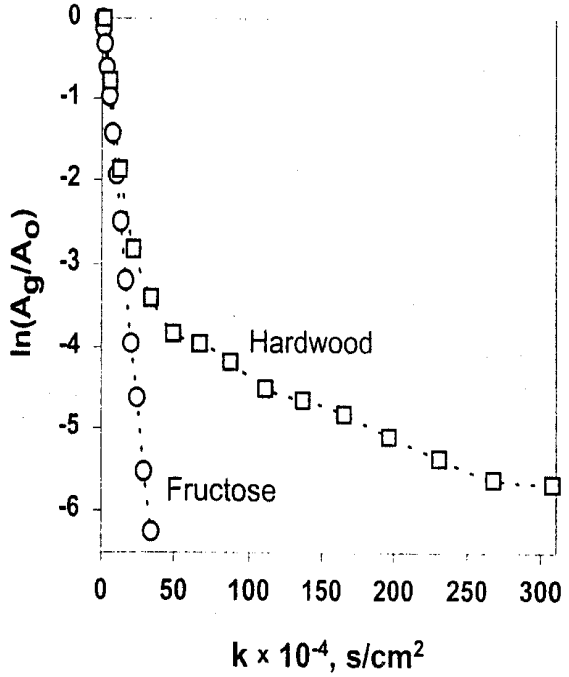

Fig. 2. Typical raw PFG-NMR data. Plot of $\ln(A_g/A_o)$ vs. k for two chars saturated with water. The squares are obtained from water diffusing in hardwood char suspensions and clearly illustrate the effects of restriction on the PFG-NMR diffusion experiment. The circles, taken from water in fructose suspensions under the same experimental conditions, represent the curve for unrestricted diffusion.

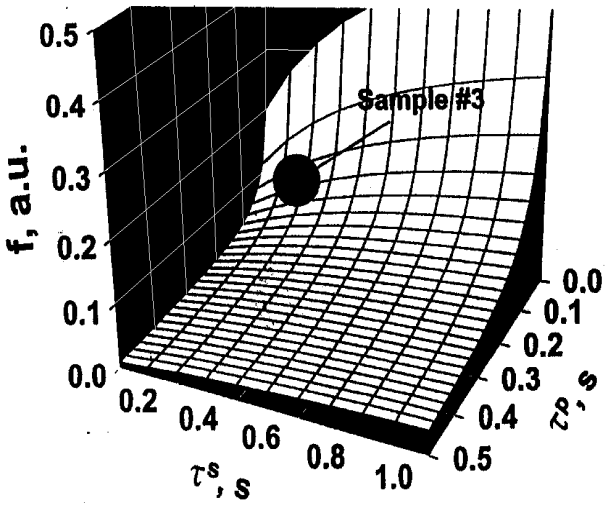

Fig. 4. The dependence of leakage factor *f* on the sticking times of τ^p and τ' for fructose char suspensions.

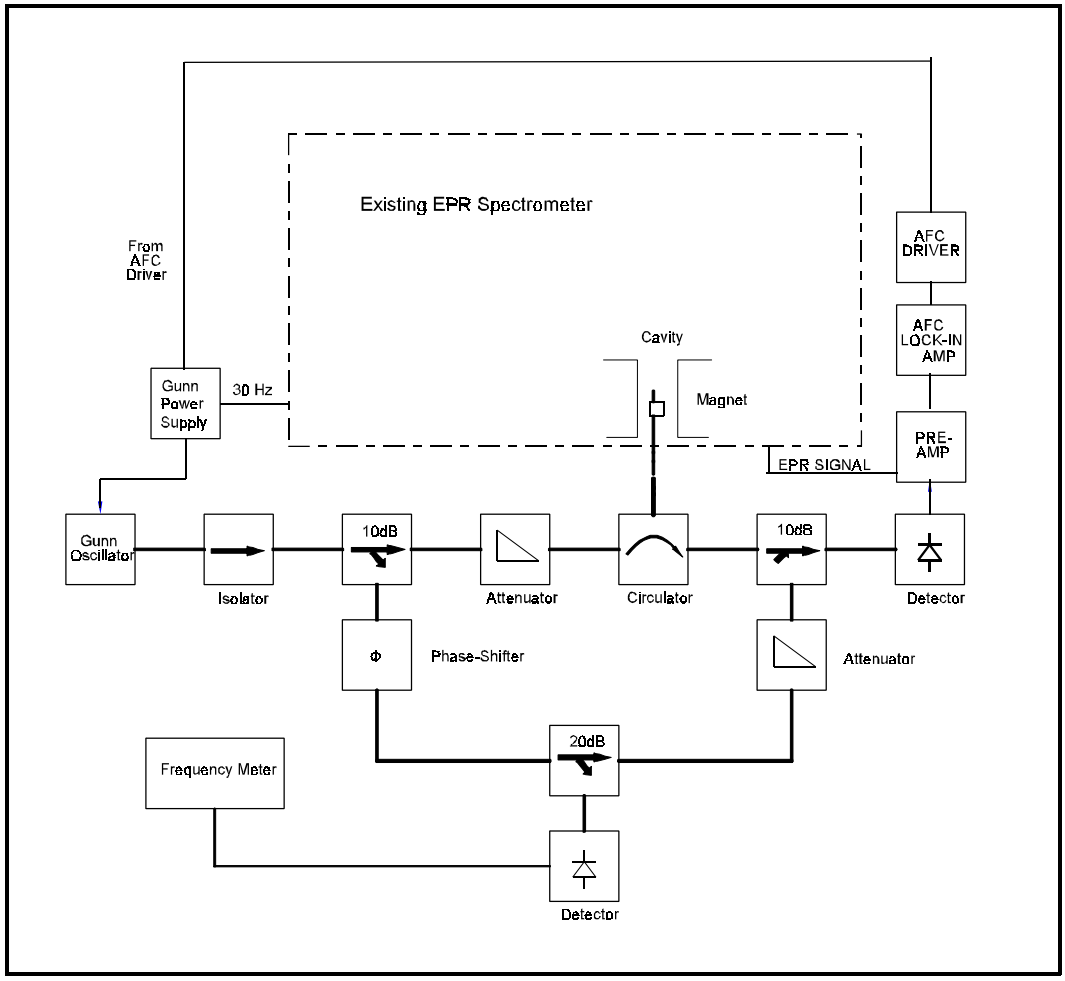

Figure 5. Block diagram of the U-band EPR spectrometer system.

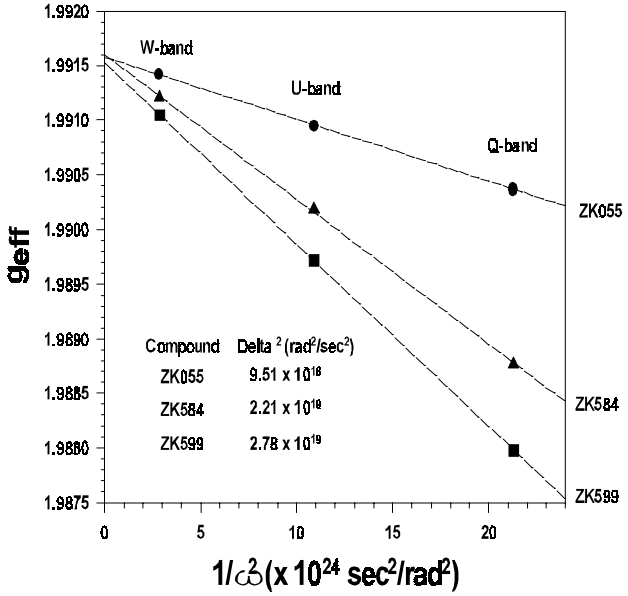

Figure 6. The effective g value (g_{eff})as a function of wavelength-squared or inverse frequency squared ($1/\nu^2$). The new U-band spectrometer fills the gap between Q-band and W-band. (Note: $\omega = 2\pi\nu$.)

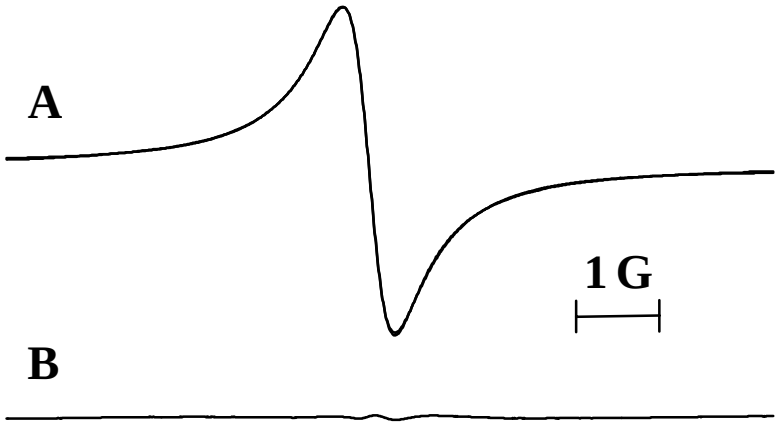

Figure 7. Experimental 9.5 GHz (X-band) EMR spectrum of deoxygenated fusinite sample and the results of least-squares simulations based on high-temperature-limit dipolar model (A), (B) is the fit residual.

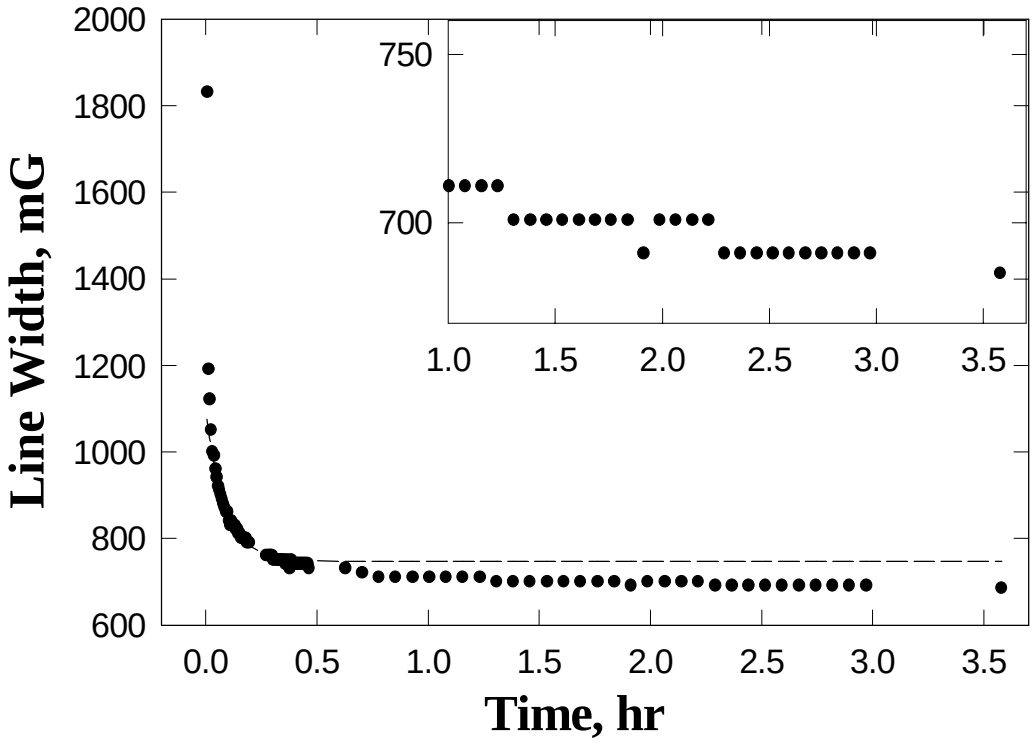

Figure 8. Kinetics of apparent peak-to-peak line width of the fusinite sample in course of continuous deoxygenation as measured at X-band.

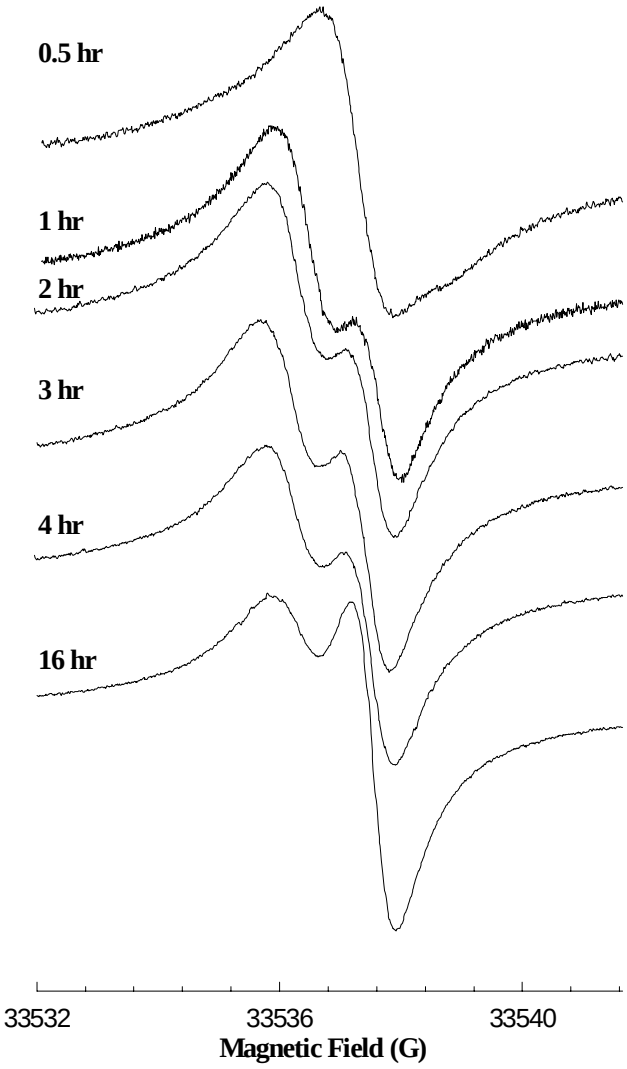

Figure 9. Gradual changes in 95 GHz EMR spectra of fusinite in course of deoxygenation

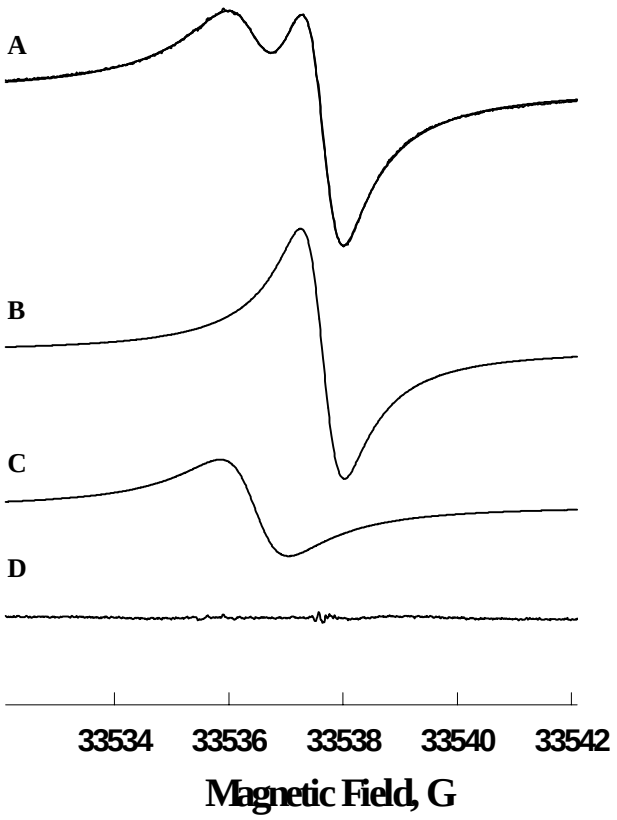

Figure 10. Experimental 95 GHz (X-band) EMR spectrum of fusinite sample deoxygenated for 16 hrs is superimposed with the results of least-squares simulations; (B) is the simulation of first component; (C) is the second component, and (D) is the fit residual.